Intramolecular Donor–Acceptor Regioregular Poly(hexylphenanthrenyl-imidazole thiophene) Exhibits Enhanced Hole Mobility for Heterojunction Solar Cell Applications

By *Yao-Te Chang, So-Lin Hsu, Ming-Hsin Su,* and *Kung-Hwa Wei**

Conjugated polymers possessing extended arrays of delocalized π electrons are being investigated intensively for their potential use in organic optoelectronic devices, with some studies focused on solar-cell devices incorporating bulk heterojunctions using conjugated polymers.[1–7] Polythiophene derivatives are at present among the most promising materials for solar-cell applications because of their high light absorption and electronic conductivity. For example, polymer solar cells containing blends of poly(3-hexylthiophene) (**P3HT**) and [6,6]-phenyl-C_{61}-butyric acid methyl ester (**PCBM**) have recently reached power conversion efficiencies of ~4–5% under standard solar conditions (AM 1.5G, 100 mW cm^{-2}, 25 °C).[8–13] If the power-conversion efficiency of these devices is to be improved further, the light absorption of the active polymer must be improved, because **P3HT** absorbed only ~20% of sunlight, that is, the band-gap of **P3HT** must be reduced to meet the maximum photon flux of sunlight. Research into conjugated polymers containing electron donor–acceptor (D–A) pairs in the polymeric main chain has recently become quite active[14] because such materials exhibit narrow band-gaps. Alternatively, the introduction of an electron-acceptor unit—usually a conjugated species that can absorb a different wavelength of sunlight—onto the side chain of a conjugated polymer can increase the breadth of wavelengths of light absorbed, and can also lower the band-gap to some extent.[15] Additionally, the generated excitons can be readily dissociated into electrons and holes in this type of conjugated polymer, because of the internal field produced by the dipole moment built on its D–A molecular structure and subsequent charge transfer to nearby *n*-type nanoparticles (for example, **PCBM**). Therefore, conjugated polymers that contain side-chain-tethered conjugated acceptor moieties not only absorb light more effectively (multiple absorption) but also exhibit enhanced charge-transfer ability—two desirable properties for photovoltaics applications.[16] In a heterojunction polymer solar cell, however, the photocurrent depends not only on the rate of photogeneration of free electrons and holes but also on the transport properties of the electrons and holes in the acceptor and donor, respectively. In fact, the overall performance of bulk-heterojunction solar cells is directly limited by the ambipolar carrier transport.[17,18] In the **P3HT/PCBM** system, the slower rate of hole transport governs the recombination process;[19] increasing the carrier mobilities results in both increased extraction of the charge carriers and increased bimolecular recombination.[20] Therefore, the incorporation of electron-withdrawing moieties as side chains that are conjugated with the polymeric main chains should also alleviate the recombination problem, because such a molecular architecture has the advantage in a heterojunction device of allowing charge separation through sequential transfer of electrons from the main chains to the side chains and then to **PCBM**. Hence, in this present study, we synthesized a new kind of intramolecular D–A thiophene-type homopolymer presenting phenanthrenyl-imidazole moieties. Scheme 1 displays our synthetic approach toward the planar phenanthrenyl-imidazole moiety-tethered thiophene monomer and its polymerization. We expected that the presence of the hexylphenanthrenyl-imidazole moieties conjugated to the thiophene units would reduce the band-gap of the polythiophene, and that the hexyl substituents would improve the solubility of the polymer. The extent of reduction of the band-gap of our synthesized polymer would, however, depend on the effective conjugation length of the system, which is sometimes reduced by steric hindrance.[21] We polymerized the 2-(2,5-dibromothiophen-3-yl)-6,9-dihexyl-1-(4-hexylphenyl)-1*H*-phenanthro-[9,10-d]-imidazole (**HPIT**) monomer using a Grignard metathesis approach. The presence of the bulky hexylphenanthrenyl-imidazole unit appended to the thiophene monomer led to very high selectivity during the Grignard reaction, resulting in highly regioregular poly(hexylphenanthrenyl-imidazole thiophene) (**PHPIT**). The number molecular weight (M_n) of **PHPIT** was 15.3 kg mol^{-1}, and the polydispersity index (PDI) was 1.35, indicating that **PHPIT** possessed ~20 repeating units. The 5% thermal degradation temperature of this polymer was 355 °C.

Figure 1 displays the UV–vis spectra of **PHPIT/PCBM** (1:1, w/w) and the **P3HT/PCBM** (1:1, w/w) solid film obtained after annealing at 120 °C for 30 min, as well as cyclic voltammogram (CV) band-gap data for **PHPIT**, PEDOT, **PCBM**, Al, and ITO. The peak at 305 nm was caused by the presence of conjugated phenanthrenyl-imidazole moieties that were not fully coplanar with the polythiophene chain due to steric hindrance. The maximum absorption (λ_{max}) at ~12 nm for the **P3HT/PCBM** thin film resulted from π–π* transitions. The annealed **PHPIT/PCBM**

[*] Prof. K. H. Wei, Y. T. Chang, S. L. Hsu, M. H. Su
Department of Materials Science and Engineering
National Chiao Tung University
1001 Ta Hsueh Road
Hsinchu, 30049 Taiwan (R.O.C.)
E-mail: khwei@mail.nctu.edu.tw

DOI: 10.1002/adma.200802379

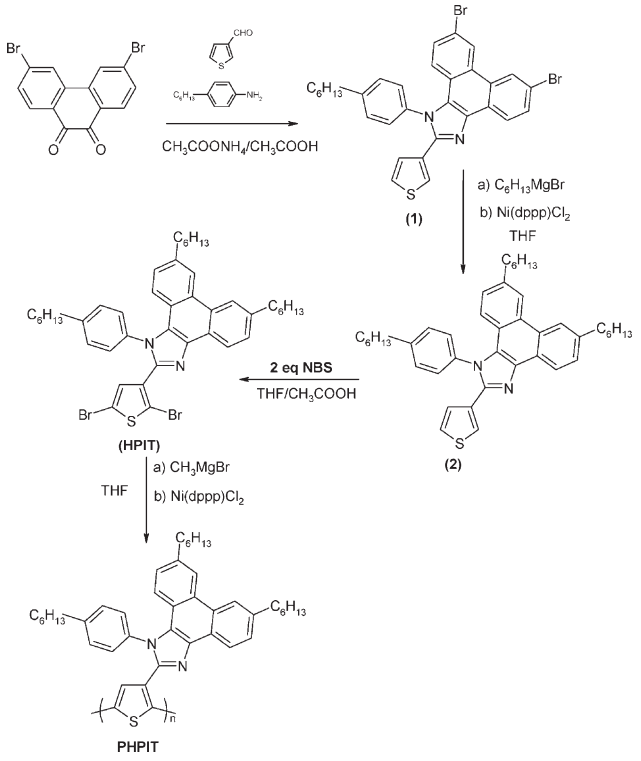

Scheme 1. Synthesis of the monomer and polymer; NBS: *N*-bromosuccinimide; THF: tetrahydrofuran; dppp: 1,3-bis(diphenylphosphino) propane.

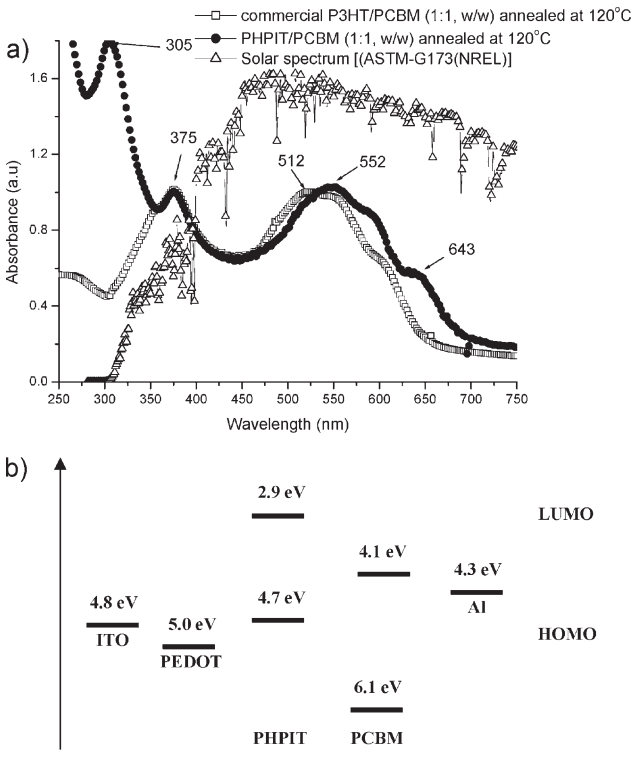

Figure 1. a) UV–vis spectra of **P3HT/PCBM** as cast and **PHPIT/PCBM** annealed at 120 °C in the solid state, and the solar spectrum. b) CV band-gap data for **PHPIT**, PEDOT, **PCBM**, Al, and ITO.

film exhibits a red-shift π–π* transition peak at 552 nm and two additional absorption peaks at 596 and 641 nm, indicating that a phase-separated structure developed after annealing at 120 °C. The area under the spectrum in the visible absorption range (400–750 nm) for **PHPIT/PCBM** after annealing at 120 °C for 30 min was 11% higher than that of the annealed **P3HT/PCBM**. The optical band-gap of **PHPIT** was ~1.85 eV, which is close to the cyclic voltammogram (CV) band-gap (1.80 eV), with the highest occupied molecular orbital (HOMO) at ~4.70 eV and the lowest unoccupied molecular orbital (LUMO) at ~2.90 eV. We detected no photoluminescence from the **PHPIT** film, suggesting that charge transfer from the photoexcited polythiophene backbone to the electron-withdrawing phenanthrenyl-imidazole side chains was sufficiently rapid to compete with radiative recombination of the excitons.[15,22]

Figure 2 displays the photocurrents of diodes with the structure ITO/PEDOT:PSS/polymer: **PCBM** (1:1, w/w)/Ca/Al that were illuminated at 100 mW cm^{-2} under AM 1.5G and their dark currents. Table 1 lists the short-circuit current densities (J_{sc}), open-circuit voltages, and power conversion efficiencies of these heterojunction polymer solar cells. The value of J_{sc} for the device incorporating the **PHPIT/PCBM** blend improved to 11.3 mA cm^{-2} from 8.3 mA cm^{-2} after the annealing time at 120 °C was increased from 20 to 30 min, probably because of improved ordering of the blend structure. However, the value of J_{sc} of the device decreased to 7.8 mA cm^{-2} when the blend underwent thermal treatment at 120 °C for 45 min, probably because of decomposition of the polymer structure. Figure S2 (Supporting Information (SI)) presents the device characteristics of the blends that we subjected to annealing at temperatures of 130 and 150 °C. Among all of the systems we studied, the **PHPIT/PCBM** blend thermally treated at 120 °C for 30 min exhibited the highest power-conversion efficiency. From atomic force microscopy images (Fig. S3, SI), we found that the root-mean-square roughness of the **PHPIT/PCBM** film (2.27 nm) annealed at 120 °C for 30 min was larger than those (1.94 and 1.76 nm) of the films annealed at 120 °C for 20 and 45 min. Hence, we suspect that the rough surface effectively reduced the charge-transport distance while providing a nanoscale texture that further enhanced internal light absorption.[11b,23,24b] The power-conversion efficiency of the device incorporating **PHPIT/PCBM**

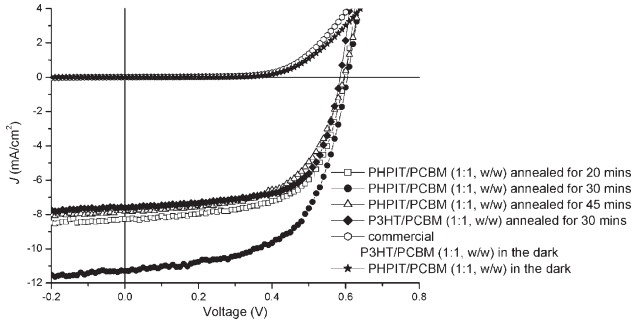

Figure 2. Current–voltage characteristics of illuminated (AM 1.5G, 100 mW cm^{-2}) polymer/**PCBM** (1:1, w/w) solar cells.

Table 1. Photovoltaic properties of polymer solar cells annealed at 120 °C for various lengths of time and of P3HT/PCBM annealed at 120 °C for 30 min.

Blend annealing at 120 °C	V_{oc} [V]	J_{sc} [mA cm^{-2}]	Fill Factor [%]	PCE [%]
PHPIT/PCBM (1:1, w/w) for 20 min	0.6	8.3	62	3.1
PHPIT/PCBM (1:1, w/w) for 30 min	0.61	11.3	60	4.1
PHPIT/PCBM (1:1, w/w) for 45 min	0.61	7.8	58	2.7
P3HT/PCBM (1:1, w/w) for 30 min	0.58	7.6	66	2.9

increased dramatically to 4.1% from 3.1% when the annealed time at 120 °C was increased from 30 to 20 min, but it decreased to 2.7% when annealed for 45 min, presumably because of decomposition of the polymer.[12c,24] We performed a control experiment in which we subjected commercially available high-molecular-weight **P3HT** ($M_n = \sim 33\,000$, about 200 repeating units) to the same annealing conditions as those experienced by **PHPIT**. The power-conversion efficiency of the device incorporating commercially available **P3HT** and **PCBM** was 2.9% (Fig. 2). Thus, although thermal treatment at 120 °C for 30 min is optimal for **PHPIT/PCBM**, that is not necessarily the case for commercial **P3HT/PCBM**.

We investigated the photophysics of the devices incorporating the synthesized copolymers by determining their external quantum efficiencies (EQEs). Figure 3 displays the EQEs of the **PHPIT/PCBM** devices in which the blends were annealed at 120 °C for various annealing times. At wavelengths from 400 to 650 nm, the absolute EQEs of the device prepared from **PHPIT/PCBM** annealed at 120 °C for 30 min were ~20% higher than those of the corresponding blends annealed for 20 and 45 min. For example, the EQE at an incident wavelength of 400 nm for the device incorporating **PHPIT/PCBM** annealed at 120 °C for 30 min improved from 53% to 79% for the corresponding device annealed for 20 min—an increase of 50%. The maximum EQEs at 460 nm for the devices containing **PHPIT** annealed at 120 °C for 30 and 20 min device were 80 and 52%, respectively—a 53% increase for the former over the latter; at a much longer wavelength of 620 nm, the corresponding values were 48 and 30%, respectively—almost a 60% increase.

Figure 4 displays the dark *J–V* curves for electron- and hole-dominated carrier devices. The electron and hole mobilities were determined by fitting the dark *J–V* curves into the space-charge-limited current (SCLC) model for electron- and hole-dominated carrier devices based on the equation

$$J = \frac{9\varepsilon_o\varepsilon_r\mu_{h(e)}V^2}{8L^3} \quad (1)$$

where ε_o is the permittivity of free space, ε_r is the dielectric constant of the polymer, $\mu_{h(e)}$ is the hole (electron) mobility, V is the voltage drop across the device, and L is the polymer

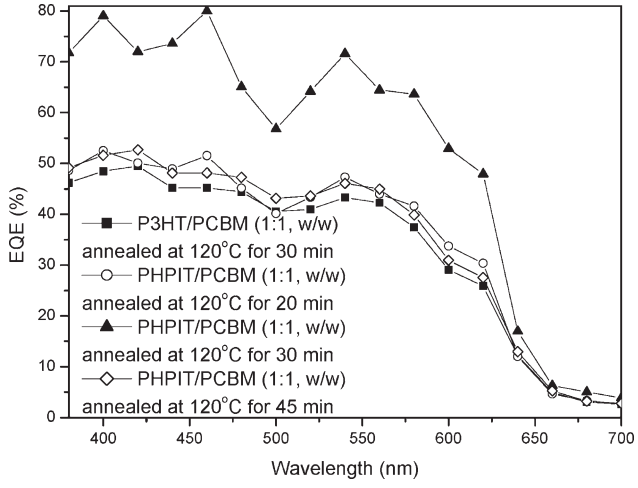

Figure 3. EQEs of devices containing polythiophene side-chain-tethered hexylphenanthrenyl-imidazole/**PCBM** blends (1:1, w/w) annealed at 120 °C for various times.

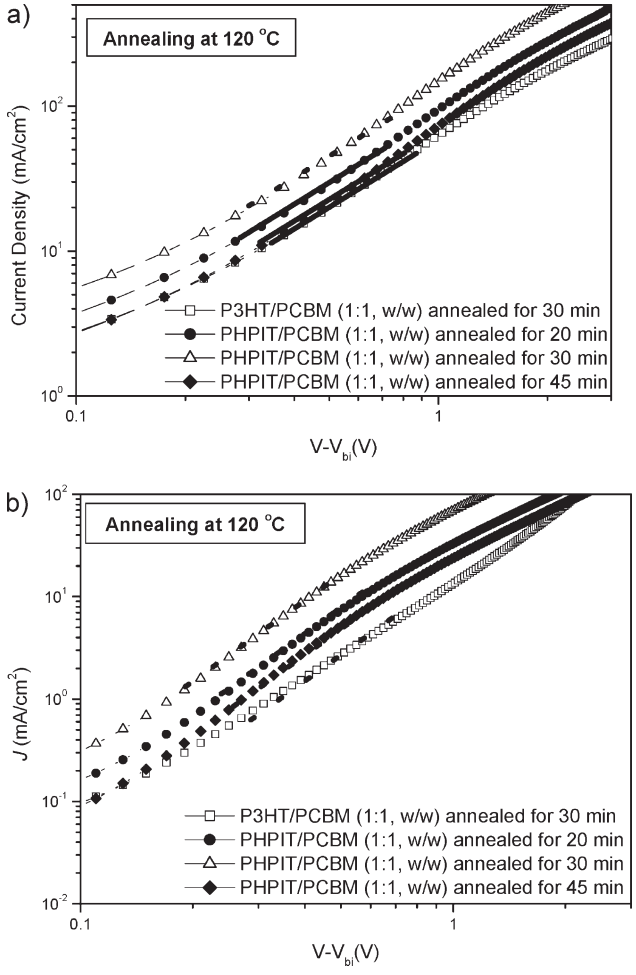

Figure 4. Dark *J–V* curves for a) electron- and b) hole-dominated carrier devices incorporating **PHPIT/PCBM** (1:1, w/w) annealed at 120 °C for various times.

Table 2. Hole mobilities, electron mobilities, and hole-to-electron-mobility ratios of P3HT/PCBM annealed at 120 °C for 30 min and PHPIT/PCBM annealed at 120 °C for various lengths of time.

Blend annealing at 120 °C	Hole mobility [μ_h, $cm^2\ Vs^{-1}$]	Electron mobility [μ_e, $cm^2\ Vs^{-1}$]	[μ_e/μ_h]
P3HT/PCBM (1:1, w/w) for 30 min	$1.8 \pm 0.1 \times 10^{-6}$	$1.8 \pm 0.1 \times 10^{-5}$	10
PHPIT/PCBM (1:1, w/w) for 20 min	$9.0 \pm 0.3 \times 10^{-6}$	$2.6 \pm 0.1 \times 10^{-5}$	2.9
PHPIT/PCBM (1:1, w/w) for 30 min	$1.9 \pm 0.1 \times 10^{-5}$	$4.2 \pm 0.1 \times 10^{-5}$	2.2
PHPIT/PCBM (1:1, w/w) for 45 min	$6.5 \pm 0.1 \times 10^{-6}$	$2.1 \pm 0.1 \times 10^{-5}$	3.2

thickness.[25] Table 2 lists the hole mobilities, electron mobilities, and the ratio of hole and electron mobilities that are determined from Figure 4 and Equation (1). We obtained hole mobilities for the **PHPIT/PCBM** system (from 6.5×10^{-6} to $1.9 \times 10^{-5}\ cm^2\ V^{-1}\ s^{-1}$) that were ~three to ten times greater than that of the **P3HT/PCBM** system ($1.8 \times 10^{-6}\ cm^2\ V^{-1}\ s^{-1}$) when both blends experienced the same thermal treatment. The device containing the **PHPIT/PCBM** blend annealed at 120 °C for 30 min exhibited the highest mobility, indicating that more-ordered **PHPIT/PCBM** films facilitate hole transport. Thus, the lowest electron-to-hole mobility ratio for the **PHPIT/PCBM** blend results in the highest photocurrent.[11b]

In summary, we have synthesized **PHPIT**, a new kind of intramolecular D–A side-chain-tethered hexylphenanthrenyl-imidazole polythiophene. The visible-light absorption of the **PHPIT/PCBM** blend is enhanced by the presence of the electron-withdrawing hexylphenanthrenyl-imidazole. The EQE of the device was maximized when the **PHPIT/PCBM** blend experienced annealing at 120 °C for 30 min. The more-balanced electron and hole mobilities and the enhanced visible- and internal-light absorptions in the devices consisting of annealed **PHPIT/PCBM** blends both contributed to a much higher short-circuit current density, which in turn led to a power-conversion efficiency as high as 4.1%, despite the fact that **PHPIT** is only comprised of ~20 repeating units.

Experimental

Materials: Chemicals were purchased from Aldrich, TCI, or Lancaster. **PCBM** was purchased from Nano-C.

Preparation of Monomers: Scheme 1 illustrates the synthetic route followed for the preparation of the monomer **HPIT**. 6,9-Dihexyl-1-(4-hexylphenyl)-3a,11b-dihydro-2-(thiophen-3-yl)-1*H*-phenanthro[9,10-d] imidazole (**2**) was isolated in 80% yield from the reaction of compound (**1**) with hexylmagnesium bromide and Ni(dppp)Cl_2 under reflux. **HPIT** was isolated in 93% yield from the reaction between **2** and NBS [15]. Detailed synthetic procedures and characterization data are provided in the Supporting Information.

Preparation of Polythiophene Derivatives [26]: The Grignard metathesis polymerization of 2-(2,5-dibromothiophen-3-yl)-1-phenyl-1*H*-phenanthro [9,10-d]-imidazole is illustrated in Scheme 1. Detailed synthetic procedures and characterization data are provided in the Supporting Information.

Characterization: ^1H and ^{13}C NMR spectra were recorded using a Varian Unity-300 NMR spectrometer. Infrared spectra were recorded from KBr disks using a Nicolet Protégé-460 FTIR spectrophotometer. Elemental analyses (EA) of the polymers were performed using a Heraeus CHN-OS Rapid instrument. Thermogravimetric analyses of the polythiophene derivatives were performed using a DuPont TGA 2950 instrument operated at a heating rate of 10 °C min^{-1} under a nitrogen purge. Differential scanning calorimetry (DSC) was performed using a DuPont DSC 2010 instrument operated at a heating rate of 10 °C min^{-1} under a nitrogen purge. Samples were heated from 30 to 200 °C, cooled to 20 °C, and then heated again from 30 to 200 °C; the glass-transition temperatures (T_g) were determined from the second heating scans. The redox behavior of each polymer was investigated through cyclic voltammetry using a BAS 100 electrochemical analyzer operated at a potential scan rate of 40 mV s^{-1} and an electrolyte of 0.1 M tetrabutylammonium hexafluorophosphate (n-Bu_4NPF_6) in acetonitrile. In each case, a glassy disk carbon electrode coated with a thin layer of the polymer was used as the working electrode, a platinum wire was used as the counter electrode, and a silver wire was used as the quasi-reference electrode. All potentials quoted herein are referenced to the Ag wire as the quasi-reference electrode; the electrochemical potential of Ag is −0.02 V versus SCE. The HOMO and LUMO energy levels were determined using the equations $E_{HOMO} = -E_{ox} - 4.4$ eV and $E_{LUMO} = -E_{red} - 4.4$ eV, where E_{ox} and E_{red} are the onset potentials of the oxidation and reduction peaks (vs. saturated calomel electrode (SCE)), respectively, and the value of 4.4 eV relates the SCE reference to a vacuum[15a,19a]. UV–vis spectra were measured using an HP 8453 diode array spectrophotometer. The molecular weights of the polythiophene derivatives were measured through gel-permeation chromatography (GPC) using a Waters chromatography unit interfaced to a Waters 2414 differential refractometer. Three 5 μm Waters styragel columns were connected in series in decreasing order of pore size (10^4, 10^3, and 10^2 Å); tetrahydrofuran (THF) was the eluent, and standard polystyrene samples were used for calibration. AFM samples were prepared by spin-coating solutions of polymer/**PCBM** blends in dichlorobenzene onto ITO glass substrates, followed by annealing in an oven at 120 °C for 20, 30, or 45 min.

Device Fabrication: The current density–voltage (*J–V*) characteristics of the polymers were measured using devices with a sandwich structure (ITO/PEDOT:PSS/polymer:**PCBM** (1:1, w/w)/Ca/Al). The ITO-coated glass substrate was precleaned and treated with oxygen plasma prior to use. The polymer/**PCBM** layer was spin-coated at 700 rpm from a dichlorobenzene solution (20 mg mL^{-1}). Dichlorobenzene was a better solvent for these polymers than were toluene, chloroform, and THF. The thickness of the polymer/**PCBM** layer was ~100 nm. The active layers of our devices were thermally annealed at 120 °C for 30 min prior to electrode deposition. Using a base pressure below 1×10^{-6} torr (1 torr = 133.32 Pa), a layer of Ca (30 nm) was vacuum-deposited as the cathode and then a thick layer of Al (100 nm) was deposited as the protecting layer; the effective area of one cell was 0.04 cm^2. Testing of the devices was performed under simulated AM 1.5G irradiation (100 mW cm^{-2}) using a xenon lamp-based Newport 66902 150W solar simulator. A xenon lamp equipped with an AM1.5 filter was used as the white-light source; the optical power at the sample was 100 mW cm^{-2}, detected using an OPHIR thermopile 71964. The *J–V* characteristics were measured using a Keithley 236 electrometer. The spectrum of the solar simulator had a mismatch of less than 25%; it was calibrated using a PV-measurement (PVM-154) mono-Si solar cell (NREL calibrated), and a Si photodiode (Hamamatsu S1133) was employed to check the uniformity of the exposed area. AM 1.5G (ASTM G173) [27] light intensity was calibrated through thermopile and PV-measurements. The mismatch factor (M) of 1.34 was obtained by taking the PVM-154 as the reference cell. The PVM-154 combined with a KG-5 filter (350–700 nm passed, Newport) was used to simulate a reference solar cell exhibiting spectral responsivity from 350 to 700 nm. Reported efficiencies are the averages obtained from four devices prepared on each substrate. The external quantum efficiency (EQE) was measured using a Keithley 236

electrometer coupled with an Oriel Cornerstone 130 monochromator. The light intensity at each wavelength was calibrated using an OPHIR 71580 diode. Hole-only devices, used to investigate the hole transport in polymer/**PCBM**, were fabricated following the same procedure presented above, except that the top electrode was replaced with gold (Au, 100 nm). Electron-only devices were fabricated by spin-coating the active layer on top of glass/Ag (100 nm) followed by evaporation of the Al (100 nm) top electrode. The *J–V* curve was measured using a Keithley 236 electrometer under inert condition.

Acknowledgements

We are grateful for the financial support provided by the National Science Council through Project NSC 96-2120-M-009-005. We thank H.-S. Wang for assisting in the synthesis of the polymers and C.-C. Chen for assisting in the study of devices of this paper. Supporting Information is available online from Wiley InterScience or from the author.

Received: August 15, 2008
Revised: January 16, 2009
Published online: March 2, 2009

[1] a) C. Ego, D. Marsitzky, S. Becker, J. Zhang, A. C. Grimsdale, K. Müllen, J. D. MacKenzie, C. Silva, R. H. Friend, *J. Am. Chem. Soc.* **2003**, *125*, 437. b) J. Pei, W. Yu, J. Ni, Y. Lai, W. Huang, A. J. Heeger, *Macromolecules* **2001**, *34*, 7241. c) F. Zhang, E. Perzon, X. J. Wang, W. Mammo, M. R. Andersson, O. Inganäs, *Adv. Funct. Mater.* **2005**, *15*, 745. d) O. Inganäs, M. Svensson, F. Zhang, A. Gadisa, N. K. Persson, X. Wang, M. R. Andersson, *Appl. Phys. A: Mater. Sci. Process.* **2004**, *79*, 31. e) F. Zhang, M. Svensson, M. R. Andersson, M. Maggini, S. Bucella, E. Menna, O. Inganäs, *Adv. Mater.* **2001**, *13*, 1871. f) A. Marcos Ramos, M. T. Rispens, J. K. J. Van Duren, J. C. Hummelen, R. A. J. Janssen, *J. Am. Chem. Soc.* **2001**, *123*, 6714. g) F. Giacalone, N. Martin, *Chem. Rev.* **2006**, *106*, 5136. h) X. Wang, E. Perzon, F. Oswald, F. Langa, S. Admassie, M. R. Andersson, O. Inganäs, *Adv. Funct. Mater.* **2005**, *15*, 1665. i) X. J. Wang, E. Perzon, J. L. Delgado, P. de la Cruz, F. Zhang, F. Langa, M. R. Andersson, O. Inganäs, *Appl. Phys. Lett.* **2004**, *85*, 5081. j) M. Y. Chiu, U. S. Jeng, C. H. Su, K. S. Liang, K. H. Wei, *Adv. Mater.* **2008**, *20*, 2573. k) J. Huang, G. Li, Y. Yang, *Adv. Mater.* **2008**, *20*, 415. l) R. J. Tseng, R. Chan, V. C. Tung, Y. Yang, *Adv. Mater.* **2008**, *20*, 435.

[2] J. H. A. Smits, S. C. J. Meskers, R. A. J. Janssen, A. W. Marsman, D. M. D. Leeuw, *Adv. Mater.* **2005**, *17*, 1169.

[3] G. Yu, J. Gao, J. C. Hummelen, F. Wudl, A. J. Heeger, *Science* **1995**, *270*, 1789.

[4] a) W. U. Huynh, J. J. Dittmer, A. P. Alivisatos, *Science* **2002**, *295*, 2425. b) J. Liu, E. N. Kadnikova, Y. Liu, M. D. McGehee, J. M. J. Fréchet, *J. Am. Chem. Soc.* **2004**, *126*, 9486. c) J. Liu, T. Tanaka, K. Sivula, A. P. Alivisatos, J. M. J. Fréchet, *J. Am. Chem. Soc.* **2004**, *126*, 6550.

[5] K. M. Coakley, M. D. McGehee, *Chem. Mater.* **2004**, *16*, 4533.

[6] T. J. Savenije, J. E. Kroeze, X. Yang, J. Loos, *Adv. Funct. Mater.* **2005**, *15*, 1260.

[7] Y. Liu, M. A. Summers, C. Edder, J. M. J. Fréchet, M. D. McGehee, *Adv. Mater.* **2005**, *17*, 2960.

[8] V. D. Mihaiketchi, H. Xie, B. D. Boer, L. J. A. Koster, P. W. M. Blom, *Adv. Funct. Mater.* **2006**, *16*, 699.

[9] J. Hou, Z. Tan, Y. Yan, Y. He, C. Yang, Y. F. Li, *J. Am. Chem. Soc.* **2006**, *128*, 4911.

[10] K. Sivula, Z. T. Ball, N. Watanabe, J. M. J. Fréchet, *Adv. Mater.* **2006**, *18*, 206.

[11] a) G. Li, V. Shrotriya, Y. Yao, Y. Yang, *J. Appl. Phys.* **2005**, *98*, 043704. b) G. Li, V. Shrotriya, J. Huang, Y. Yao, T. Moriarty, K. Emery, Y. Yang, *Nat. Mater.* **2005**, *4*, 864. c) G. Li, Y. Yao, H. Yang, V. Shrotriya, G. Yang, Y. Yang, *Adv. Funct. Mater.* **2007**, *17*, 1636.

[12] a) T. Erb, U. Zhokhavets, G. Gobsch, S. Raleva, B. Stühn, P. Schilinsky, C. Waldauf, C. J. Brabec, *Adv. Funct. Mater* **2005**, *15*, 1193. b) J. Y. Kim, K. Lee, N. E. Coates, D. Moses, T.-Q. Nguyen, M. Dante, A. J. Heeger, *Science* **2007**, *317*, 222. c) W. Ma, C. Yang, X. Gong, K. Lee, A. J. Heeger, *Adv. Funct. Mater.* **2005**, *15*, 1617. d) M. Reyes-Reyes, K. Kim, D. L. Carrolla, *Appl. Phys. Lett.* **2005**, *87*, 83506.

[13] I. Riedel, E. V. Hauff, J. Parisi, N. Martin, F. Giacalone, V. Dyakonov, *Adv. Funct. Mater.* **2005**, *15*, 1979.

[14] a) C. J. Brabec, N. S. Sariciftci, J. C. Hummelen, *Adv. Funct. Mater.* **2001**, *11*, 15. b) S. C. Ng, H.-F. Lu, H. S. O. Chan, A. Fujii, T. Laga, K. Yoshino, *Adv. Mater.* **2000**, *12*, 1122. c) Z. Bao, Z. Peng, M. E. Galvin, E. A. Chandross, *Chem. Mater.* **1998**, *10*, 1201.

[15] a) Y.-T. Chang, S.-L. Hsu, M.-H. Su, K.-H. Wei, *Adv. Funct. Mater.* **2007**, *17*, 3326. b) Y.-T. Chang, S.-L. Hsu, M.-H. Su, K.-H. Wei, T.-A. Singh, E. W.-G. Diao, *Adv. Funct. Mater.* **2008**, *20*, 2573.

[16] Z. Zhu, D. Waller, R. Gaudiana, M. Morana, D. Mülhbacher, M. Scharber, C. J. Brabec, *Macromolecules* **2007**, *40*, 1981.

[17] J. I. Nakamura, K. Murata, K. Takahashi, *Appl. Phys. Lett.* **2005**, *87*, 132105.

[18] A. C. Arango, L. R. Johnson, V. N. Bliznyuk, Z. Schlesinger, S. A. Carter, H.-H. Hörhold, *Adv. Mater.* **2000**, *12*, 1689.

[19] M. M. Mandoc, L. J. A. Koster, P. W. M. Blom, *Appl. Phys. Lett.* **2007**, *90*, 133504.

[20] B. C. Thompson, J. M. J. Fréchet, *Angew. Chem. Int. Ed.* **2008**, *47*, 58.

[21] a) E. H. A. Beckers, S. C. J. Meskers, A. P. H. J. Schenning, Z. Chen, F. Würthner, P. Marsal, D. Beljonne, J. Cornil, R. A. J. Janssen, *J. Am. Chem. Soc.* **2006**, *128*, 649. b) A. M. Ramos, S. C. J. Meskers, E. H. A. Beckers, R. B. Prince, L. Brunsveld, R. A. J. Janssen, *J. Am. Chem. Soc.* **2004**, *126*, 9630.

[22] F. Giacalone, J. L. Segura, N. Martin, M. Catellani, S. Luzzati, N. Lupsac, *Org. Lett.* **2003**, *5*, 1669.

[23] S. Berson, R. D. Bettignies, S. Bailly, S. Guillerez, *Adv. Funct. Mater.* **2007**, *17*, 1377.

[24] a) F. Padinger, R. S. Rittberger, N. S. Sariciftci, *Adv. Funct. Mater.* **2003**, *13*, 85. b) L. H. Nguyen, H. Hoppe, T. Erb, S. Günes, G. Gobsch, N. S. Sariciftci, *Adv. Funct. Mater.* **2007**, *17*, 1071.

[25] a) P. W. M. Blom, M. J. M. de Jong, M. G. van Munster, *Phys. Rev. B* **1997**, *55*, R656. b) C. Goh, R. J. Kline, M. D. McGehee, *Appl. Phys. Lett.* **2005**, *86*, 122110. c) C. Melzer, E. J. Koop, V. D. Mihailetchi, P. W. M. Blom, *Adv. Funct. Mater.* **2004**, *14*, 865. d) V. R. Nikitenko, H. Heli, H. V. Seggern, *J. Appl. Phys.* **2003**, *94*, 2480. e) P. W. M. Blom, M. J. M. D. Jong, J. J. M. Vleggaar, *Appl. Phys. Lett.* **1996**, *68*, 3308. f) V. D. Mihailetchi, J. Wildeman, P. W. M. Blom, *Phys. Rev. Lett.* **2005**, *94*, 126602.

[26] a) R. D. McCullough, R. D. Lowe, M. Jayaraman, D. L. Anderson, *J. Org. Chem.* **1993**, *58*, 904. b) M. C. Iovu, E. E. Sheina, R. R. Gil, R. D. McCullough, *Macromolecules* **2005**, *38*, 8649. c) E. E. Sheina, S. M. Khersonsky, E. G. Jones, R. D. McCullough, *Chem. Mater.* **2005**, *17*, 3317.

[27] American Society for Testing and Materials (ASTM) standard G173, *Standard Tables for Reference Solar Spectrum Irradiance: Direct Normal and Hemispherical on 37° Tilted Surface*.